Inorg. Chem. **XXXX**, *xx*, 0

A Unique Family of Stable and Water-Soluble *S*-Nitrosothiol Complexes

Laura L. Perissinotti,[†] Gregory Leitus,[‡] Linda Shimon,[‡] Dario Estrin,[†] and Fabio Doctorovich*[,†]

Departamento de Química Inorgánica, Analítica y Química Física/INQUIMAE, Facultad de Ciencias Exactas y Naturales, Universidad de Buenos Aires, Ciudad Universitaria, Pabellón II, (C1428EHA) Buenos Aires, Argentina, and Department of Chemical Services, The Weizmann Institute of Science, Rehovot 76100, Israel

Received December 26, 2007

In this work, we present a complete and detailed experimental characterization and theoretical study of a variety of coordinated *S*-nitrosothiols (RSNOs), such as cysteine derivatives, mercaptosuccinic acid, benzyl thiol, and phenyl thiol. Some of them are extremely unstable and sensitive in free form. Strikingly, in contrast with free S-nitrosothiols, we found that, upon coordination to iridium, they become very stable even in aqueous solutions. The study of these coordinated complexes provides further insight on the elucidation of structural aspects dealing with the nature of the S−N bond in RSNOs, a fact which still remains a matter of controversy.

Introduction

S-nitrosothiols (RSNOs) have been steadily attracting increasing interest in view of their role *in vivo* as potential biocatalysts and reagents for the storage and transport of nitric oxide.[1] For that reason, the chemistry and biochemistry of *S*-nitrosothiols have been surveyed several times.[2–6]

In general, RSNO compounds may be prepared from treatment of the precursor thiol (RSH) with nitrosating agents,[7] including nitric oxide in the presence of electron acceptors, nitrosonium salts, nitrous acid, inorganic nitrites, metal nitrosyl complexes, and many others.[5] In the cases when the nitrosating agent is a metal nitrosyl, the thiol interacts with the nitrosyl ligand, forming an *S*-nitrosothiol ligand (N(O)SR) coordinated to the metal center, {M−N(O)SR}.

A long- and well-established method that has been used to prepare nitrosothiols complexes *in situ*[8–11] consists of the reaction of a free thiolate anion and the ligand NO^+ coordinated to $[Fe(CN)_5]^{3-}$ or other coordinating moiety. This reaction of nitroprusside with thiols has been extended to a great variety of nitrosyl complexes of formula type $\{(X)_5MNO\}^n$, with X comprising ligands of different donor–acceptor abilities and M = Fe, Ru, and Os. In most cases, these complexes are unstable and decompose spontaneously to metal complexes and disulfides, the lifetimes depending strongly on the thiol structure.[12]

Recently, in a previous work, we presented the reaction between a free thiol, benzyl mercaptan, and $K[IrCl_5NO]$, leading to the formation of the surprisingly stable coordinated nitrosothiol *trans*-$K[IrCl_4(CH_3CN)N(O)SCH_2Ph]$.

$$K[IrCl_5NO] + PhCH_2SH \xrightarrow{CH_3CN} \textit{trans}\text{-}K[IrCl_4(CH_3CN)N(O)SCH_2Ph] + H^+ + Cl^-$$

This was the first time that a nitrosothiol complex was isolated and fully characterized, including a structural determination by X-ray crystallography. This finding repre-

* Corresponding author e-mail: doctorovich@qi.fcen.uba.ar.
† Universidad de Buenos Aires.
‡ The Weizmann Institute of Science.

(1) Williams, D. L. H. *Acc. Chem. Res.* **1999**, *32* (10), 869–876.
(2) Jourd'heuil, D.; Hallen, K.; Feelisch, M.; Grisham, M. B. *Free Radical Biol. Med.* **2000**, *28* (3), 409–417.
(3) Stamler, J. S.; Jia, L.; Eu, J. P.; McMahon, T. J.; Demchenko, I. T.; Bonaventura, J.; Gernert, K.; Piantadosi, C. A. *Science* **1997**, *276* (5321), 2034–2037.
(4) Stamler, J. S.; Jaraki, O.; Osborne, J.; Simon, D. I.; Keaney, J.; Vita, J.; Singel, D.; Valeri, C. R.; Loscalzo, J. *Proc. Natl. Acad. Sci. U. S. A.* **1992**, *89* (16), 7674–7677.
(5) Szacilowski, K.; Stasicka, Z. *Prog. React. Kinet. Mech.* **2001**, *26* (1), 1–58.
(6) Mannick, J. B.; Hausladen, A.; Liu, L. M.; Hess, D. T.; Zeng, M.; Miao, Q. X.; Kane, L. S.; Gow, A. J.; Stamler, J. S. *Science* **1999**, *284* (5414), 651–654.
(7) Oae, S.; Shinhama, K. *Org. Prep. Proced. Int.* **1983**, *15* (3), 165–198.
(8) Butler, A. R.; Calsyharrison, A. M.; Glidewell, C.; Sorensen, P. E. *Polyhedron* **1988**, *7* (13), 1197–1202.
(9) Johnson, M. D.; Wilkins, R. G. *Inorg. Chem.* **1984**, *23* (2), 231–235.
(10) Mulvey, D.; Waters, W. A. *J. Chem. Soc., Dalton Trans.* **1975**, *10*, 951–959.
(11) Szacilowski, K.; Oszajca, J.; Stochel, G.; Stasicka, Z. *J. Chem. Soc., Dalton Trans.* **1999**, *14*, 2353–2357.
(12) Szacilowski, K.; Wanat, A.; Barbieri, A.; Wasielewska, E.; Witko, M.; Stochel, G.; Stasicka, Z. *New J. Chem.* **2002**, *26* (10), 1495–1502.
(13) Perissinotti, L. L.; Estrin, D. A.; Leitus, G.; Doctorovich, F. *J. Am. Chem. Soc.* **2006**, *128* (8), 2512–2513.

10.1021/ic7024999 CCC: $40.75
Published on Web 05/09/2008

sents a good example of showing that the coordination chemistry of RSNOs uncovers new aspects of nitrosation processes; for instance, coordination to metal centers changes considerably the stability of the RSNOs.[5]

In this work, we present a complete and detailed experimental characterization and theoretical study of these novel compounds bearing a variety of coordinated nitrosothiols. This variety consists of cysteine derivaties, mercaptosuccinic acid, benzyl thiol, and phenyl thiol. The free forms of some of them are extremely unstable and sensitive. Strikingly, in contrast with free *S*-nitrosothiols, upon coordination, they become very stable even in aqueous solution.

It is important to remark that the study of these coordinated complexes is especially relevant because it allows the elucidation of structural aspects dealing with the nature of the S−N bond in RSNOs, a fact which still remains a matter of controversy.

Experimental Section

General Procedures. Materials. Potassium pentachloronitrosyl iridate(III) was purchased from Strem Chemicals, benzylmercaptan and thiophenol from Fluka, mercaptosuccinic acid and N-acetyl-L-cystein from Merk, and L-cystein ethyl ester from Sigma Aldrich; all of them were used as received.

Acetonitrile was purchased from Aldrich; it was dried with CaH_2 and distilled over it. DMSO-d_6 and D_2O were purchased from Aldrich and used as received. The water used in all reactions was MilliQ water obtained from deionized water.

NMR spectra were acquired on a Bruker AM 500 spectrometer. All measurements were carried out in D_2O and DMSO-d_6.

UV/visible absorption spectra were acquired on a Hewlett-Packard HP8453 diode array spectrometer. The half-lives were measured in milliQ water (pH = 4–5, T = 25 °C, λ = 475–581 nm) without buffering the solution (pH did not change during the decomposition).

FTIR spectra were acquired with a Nicolet Avatar FTIR spectrophotometer. Solid spectra were obtained as KBr pellets.

Mass spectrometric measurements were performed using a high-resolution hybrid quadrupole (Q) and orthogonal time-of-flight (TOF) mass spectrometer (QTof from Micromass, U.K.) operating in the negative ion electrospray ionization (ESI) mode set from 2100 to 3500 V. Samples dissolved in appropriate solvents were injected through an uncoated fused-silica capillary, using a syringe pump (Harvard Apparatus, Pump 11, 15 μL min^{-1}). The temperature of the nebulizer and desolvation gas was set at 100 °C, and the cone voltage was set between 25 and 35 V. Tandem mass spectra (ESI-MS/MS) were acquired using the product ion scan mode via mass selection of the ion of interest, followed by collision-induced dissociation (CID) with Ar using energies varying from 15 to 35 eV with high-accuracy orthogonal TOF mass analysis of the CID ionic fragments. For comparison with experimental data, isotopic patterns were calculated using the MassLynx software. Coordinated RSNOs are soluble in water, DMSO, and DMF. The solvent mixture chosen as the most appropriate for the ESI-MS experiments was a 1:1 mixture of acetonitrile and DMSO. ESI-MS and ESI-MS/MS spectra were collected using a needle voltage of 2500 V and a cone voltage of 25 V, and the collision energy was 15 eV for CID using argon as the collision gas.

All complexes were synthesized as follows: 2.28×10^{-2} mmol of corresponding thiol dissolved in 0.25 mL of acetonitrile (for the case of complexes **3a** and **4a**, a solvent mixture was used: 0.25 mL of acetonitrile + 20 μL of dried methanol) was added under an Ar atmosphere to 10 mg (2.28×10^{-2} mmol) of K[$IrCl_5$(NO)] in 0.25 mL of acetonitrile. For complexes **3a**, **4a**, and **7a**, a solvent mixture was used: 0.25 mL of acetonitrile + 20 μL of dried methanol in the case of **3a** and **4a**; in the case of **7a**, the thiol was dissolved in a minimum amount of water with a stoichiometric amount of trifluoroacetic acid. The nitrosyl iridate(III) complex is sensitive to light, so all of the procedures were carried out under light protection.

Complex 1a. K[$IrCl_5N(O)SCH_2Ph$]·$^1/_3CH_3CN$. The reaction was done at −20 °C; the product precipitated immediately as a green powder. Reaction yield: 92.0%. ^{1}H NMR (D_2O, 500 MHz): δ 4.63 (s, 2H, −C*H*$_2$−aryl), 7.34−7.40 (m, 5H, **aryl**). Elem anal. found (calcd): C, 15.9 (15.9); N, 3.3 (3.2); H, 1.6 (1.5); S, 5.4 (5.5). UV–visible [λ_{max}, nm (ϵ, M^{-1} cm^{-1})]: 328(2465), 397(4409), 511(876), 556(855). FTIR (KBr), cm^{-1}: υ_{NO} = 1431, υ_{SN} = 779.

Complex 1b. *trans*-K[$IrCl_4(CH_3CN)N(O)SCH_2Ph$]·$CH_3CN$. The reaction was done at room temperature. After some minutes, a red product precipitated. Reaction yield: 80.3%. ^{1}H NMR (D_2O, 500 MHz): δ 2.92 (s, 3H, C*H*$_3$CN−), 4.67 (s, 2H, −C*H*$_2$−aryl), 7.36–7.37 (m, 5H, **aryl**). Elem anal. found (calcd): C, 21.6 (21.7); N, 6.9 (6.9); H, 2.1 (2.1); S, 5.1 (5.3). UV–visible [λ_{max}, nm (ϵ, M^{-1} cm^{-1})]: 325(1809), 387(3283), 475(1059), 525(919). FTIR (KBr), cm^{-1}: υ_{NO} = 1432, υ_{SN} = 794.

Complex 1c. *trans*-$(P(Ph)_4)$[$IrCl_4(CH_3CN)N(O)SCH_2Ph$]·$CH_3CN$. The reaction was done in an analogous manner to that of complex **1b**. Complex **1c** was obtained by adding a saturated aqueous solution of the crude product to an ethanol saturated solution of tetraphenylphosphonium chloride. FTIR(KBr), cm^{-1}: υ_{NO} = 1436, υ_{SN} = 852.

Complex 2a. K_2[$IrCl_5N(O)SPh$]. The reaction was done at −20 °C. The product precipitated immediately as a green powder. Reaction yield: 98.8%. ^{1}H NMR (D_2O, 500 MHz): δ 7.49 (d, 2H, **aryl**), 7.65–7.76 (m, 3H, **aryl**). Elem anal. found (calcd): C, 12.2 (12.2); N, 2.5 (2.4); H, 1.0 (1.0); S, 5.4 (5.4). UV–visible [λ_{max}, nm (ϵ, M^{-1} cm^{-1})]: 337(2967), 396(4054), 506(849), 556(822). FTIR(KBr), cm^{-1}: υ_{NO} = 1438, υ_{SN} = 763.

Complex 2b. *trans*-K[$IrCl_4(CH_3CN)N(O)SPh$]·CH_3CN. The reaction was done at room temperature. After some minutes, a green-brown product precipitated. Reaction yield: 84.5%. ^{1}H NMR (D_2O, 500 MHz): δ 2.95 (s, 3H, C*H*$_3$CN−), 7.49 (s, 2H, **aryl**), 7.65–7.76 (m, 3H, **aryl**). Elem anal. found (calcd): C, 20.4 (20.2); N, 7.0 (7.1); H, 1.8 (1.8); S, 5.3 (5.3). UV–visible [λ_{max}, nm (ϵ, M^{-1} cm^{-1})]: 325(2821), 387(4728), 478(1174), 525(986). FTIR (KBr), cm^{-1}: υ_{NO} = 1453, υ_{SN} = 786.

Complex 3a. K[$IrCl_5N(O)SCH_2CH(NHCOCH_3)COOH$]. The reaction was done at −10/−20 °C. The product precipitated immediately as a green powder. Reaction yield: 82.0%. ^{1}H NMR (D_2O, 500 MHz): δ 2.0 (s, 3H, −COC*H*$_3$), 3.78–3.98 (dd, 2H, −SC*H*$_2$−), 4.65–4.70 (m, 1H, −SCH$_2$C*H*). Elem anal. found (calcd): C, 9.7 (9.9); N, 4.4 (4.6); H, 1.9 (1.5); S, 5.0 (5.3). UV–visible [λ_{max}, nm (ϵ, M^{-1} cm^{-1})]: 331(2246), 398(4375), 572(944). FTIR (KBr), cm^{-1}: υ_{NO} = 1431, υ_{SN} = 781.

Complex 4a. H[$IrCl_5N(O)SCH_2CH(COOCH_2CH_3)NH_3$]. The reaction was done at −10/−20 °C. The product precipitated immediately as a green powder. Reaction yield: 78.96%. ^{1}H NMR (D_2O, 500 MHz): δ 1.33 (t, 3H, −COOCH$_2$C*H*$_3$), 3.88–4.06 (dd, 2H, −SC*H*$_2$−), 4.36 (m, 2H, −COOC*H*$_2$−), 4.5 (t, 1H, SCH$_2$C*H*). Elem anal. found (calcd): C, 11.0 (10.9); N, 4.9 (5.1); H, 2.3 (2.2); S, 5.6 (5.8). UV–visible [λ_{max}, nm (ϵ, M^{-1} cm^{-1})]: 327(1836), 400(3235), 581(658). FTIR(KBr), cm^{-1}: υ_{NO} = 1438, υ_{SN} = 784.

Complex 5a. K_2[$IrCl_5N(O)SCH(COOH)CH_2COOH$] or KH-[$IrCl_5N(O)SCH(COOH)CH_2COOH$]. The reaction was done at

−20 °C. Immediately, a green product appeared, but its color changed to brown in a few minutes. ^{1}H NMR (DMSO-d_6, 500 MHz): δ 2.65–2.72 (m, 2H, −CH_2COOH), 4.57–4.59 (m, 1H, −SCH−). UV–visible [λ_{max}, nm (ϵ, M^{-1} cm^{-1})]: 332(2592), 401(5141), 581(1063). FTIR (KBr), cm^{-1}: υ_{NO} = 1435, υ_{SN} = 781.

Complex 6a. $K_2[IrCl_5N(O)SCH(COOCH_3)CH_2COOCH_3]\cdot$ ½CH_3CN. The reaction was done at −20 °C. After 15 min, a green product appeared. Reaction yield: 80.1%. ^{1}H NMR (DMSO-d_6, 500 MHz): δ 2.76–2.95 (m, 2H, −CH_2COO−), 3.65 (s, 6H, −COOCH_3), 4.77–4.78 (m, 1H, −SCH−). Elem anal. found (calcd): C, 12.2 (12.4); N, 2.9 (3.1); H, 1.7 (1.6); S, 5.0 (4.7). UV–visible [λ_{max}, nm (ϵ, M^{-1} cm^{-1})]: 322(4801), 397(5674), 574(1358). FTIR(KBr), cm^{-1}: υ_{NO} = 1437, υ_{SN} = 790.

Complex 7a. The reaction was done at −20 °C. To a solution of nitrosyl iridate(III) complex was added the solution containing the thiol, resulting in a color change to green. After centrifugation, the solution became separated into two phases; the aqueous phase containing the product was poured over cooled acetone, and the green product precipitated. ^{1}H NMR (D_2O (40μL) + CD_3CN (0.5 mL), 500 MHz): δ 2.08–2.23 (m, 2H, −CH_2CH(NH_2)−), 2.38–2.49 (m, 2H, −NH(CO)CH_2−), 3.60–3.80 (dd, 2H, −SCH_2−), 3.89 (d, 2H, −CH_2COOH), 4.10 (m, 1H, −SCH_2CH−), 4.73 (m, 1H, −CH(NH_2)COOH). UV–visible [λ_{max}, nm (ϵ, M^{-1} cm^{-1})]: 329, 398, 510, 573. FTIR (KBr), cm^{-1}: υ_{NO} = 1422, υ_{SN} = 770.

All ^{15}N labeled complexes, that is, $K_2[IrCl_5{}^{15}N(O)SR]$ and *trans*-$K[IrCl_4(CH_3CN)^{15}N(O)SR]\cdot CH_3CN$, were obtained in an analogous manner, using $K[IrCl_5(^{15}NO)]$ prepared from $Na^{15}NO_2$ and $K_3[IrCl_6]$ according to literature procedures. [14]In order to avoid decomposition of the $K[IrCl_5(^{15}NO)]$ complex and increase the obtained yield, a modification from the literature procedure was made. Instead of washing the labeled complex with methanol and ether as suggested, we dissolved it in dry acetonitrile; separated the sodium salt, which is not soluble in this solvent; concentrated the complex under argon; and finally precipitated it with dry toluene. The pentachloronitrosyl iridate(III) complex is light-sensitive, so all of the procedures were done under light protection.

X-ray Analysis for Structures 1b, 1c, and 8. Complex **1b** was crystallized from CH_3CN at room temperature to give red crystals. Crystal **1c** was obtained by adding a saturated aqueous solution of the crude product to an ethanol-saturated solution of tetraphenylphosphonium chloride. After slow evaporation of the supernatant, green crystals appeared. Complex **8** (orange crystals) was obtained by leaving complex **2b** dissolved in acetonitrile for several weeks. The crystals were mounted on the nylon loop and flash-frozen in a nitrogen stream at 120 K. Data were collected on a Nonius KappaCCD diffractometer mounted on an FR590 generator equipped with a sealed tube with Mo Kα radiation (λ = 0.710 73 Å) and a graphite monochromator. The structures were solved using direct methods with SHELXS-97 and refined by the full-matrix least-squares technique with SHELXS-97 based on F^2.

Complex 1b. Formula min, M_r = 608.40, specimen 0.3 × 0.3 × 0.02 mm, monoclinic, space group $P2(1)/n$, a = 17.548(4) Å, b = 6.8190(14) Å, c = 18.261(4) Å, β = 115.40(3)°, F(000) = 1152, V =1972.8(7) Å^3, T = 120(2) K, Z = 4, Dc = 2.047 mg/m^3, μ = 7.624 mm^{-1}. Refinement method: full-matrix least squares on F^2, R = 0.0447, Rw = 0.0691 (observed data with $I > 2\sigma(I)$).

Complex 1c. Formula min, M_r = 899.67, specimen 0.60 × 0.30 × 0.10 mm, triclinic, space group $P\bar{1}$, a =20.053(2) Å, b = 7.2500(5) Å, c = 26.738(3) Å, β = 104.463(3)°, F(000) = 1176, V = 3764.1(6) Å^3, T = 120(2) K, Z = 8, Dc = 1.178 mg/m^3, μ = 7.393 mm^{-1}. Refinement method: full-matrix least squares on F^2, R = 0.0700, Rw = 0.1962 (observed data with $I > 2\sigma(I)$).

Complex 8. Formula min, M_r = 537.32, specimen 0.20 × 0.20 × 0.05 mm, orthorhombic, space group *Pbca*, a = 7.5310(2) Å, b = 19.3820(6) Å, c = 23.7470(7) Å, β = 104.463(3)°, F(000) = 2016, V = 3466.25(17) Å^3, T = 120(2) K, Z = 8, Dc = 2.059 mg/m^3, μ = 8.549 mm^{-1}. Refinement method: full-matrix least squares on F^2, R = 0.0576, Rw = 0.0802 (observed data with $I > 2\sigma(I)$).

Theoretical Calculations. All calculations performed in this work were carried out using the Gaussian03 package.[15] Geometry optimizations were carried out at the PBE1PBE/SDD level of theory; this functional proved to yield results of higher quality compared to the previously used mPW1k.[16] On the optimized structures, single-point energy calculations at the PBE1PBE/SDB-cc-pVDZ level of theory were performed, to increase the accuracy of the results. Each stationary point in the gas phase was characterized by performing a normal modes analysis.

Solvent effects were modeled using the polarized continuum model (PCM)[17] scheme. The PCM implementation, in which the self-consistency between solute wave function and solvent polarization is achieved during the self-consistent field cycle, has been employed.

Results and Discussion

1. Reaction of K[IrCl$_5$NO] with Thiols: Synthesis and Structure. Free RSNOs are usually thermally unstable and undergo spontaneous decomposition, while iridium-coordinated ones turn out to be very stable even in water. It is known that, for free RSNOs, their stability is affected by the thiol alkyl chain structure, operating mainly via electronic effects, through electron-releasing or -withdrawing substituents.[5] In this regard, we decided to synthesize different coordinated RSNOs in order to evaluate the effect of the thiol structure on their stability and reactivity.

In all cases, it was found that, when the thiol was added to an acetonitrile solution of K[IrCl$_5$(NO)] in the dark, at room temperature, immediate formation of the corresponding coordinated nitrosothiol was observed as a precipitate, of which product and color depend on the reactioning thiol and temperature. All products obtained turned out to be very soluble in water. Most of them are very stable in the solid form and in solution.

Acetonitrile selection as reaction solvent lay in the fact that the reactant complex K[IrCl$_5$NO] did not decompose or react with the solvent during the reaction time in the absence of light.

As can be seen in Scheme 1, complexes **b** have an acetonitrile molecule coordinated to the trans position. The coordination of acetonitrile in the trans possition resulted as a consequence of the labilization of the corresponding chloride, which is replaced by a molecule of acetonitrile when the reaction takes place in this solvent.

(14) Bottomley, F.; Clarkson, S. G.; Tong, S. B. *J. Chem. Soc., Dalton Trans.* **1974**, (21), 2344–2346.

(15) Frisch, M. J. et al. *Gaussian03*, Revision C.02; Gaussian, Inc.: Wallingford, CT, 2004. See Supporting Information for remaining authors.

(16) Quintal, M. M.; Karton, A.; Iron, M. A.; Boese, A. D.; Martin, J. M. L. *J. Phys. Chem. A* **2006**, *110* (2), 709–716.

(17) Cossi, M.; Barone, V.; Cammi, R.; Tomasi, J. *Chem. Phys. Lett.* **1996**, *255* (4–6), 327–335.

Scheme 1

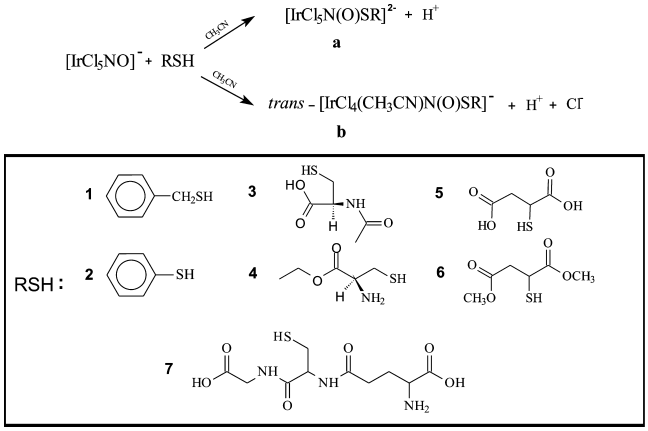

It should be noted that most of these complexes are easily obtained in excellent yields (80–99%), except for the case of **5**; where unidentified products were also obtained.

Thiols with Aromatic Rings. In the case of thiols with aromatic rings (benzylmercaptan and phenylthiol), both products were observed, complex **b** as a red precipitate and complex **a** as a green precipitate (not soluble in acetonitrile). The ratio of products obtained depends mainly on the reaction temperature. When the reaction was carried out at room temperature, the product obtained was only complex **b**, but when the reaction was done at low temperatures (−20 °C), a green precipitate immediately appeared (complex **a**).

When the reactioning thiol was benzylmercaptan, the complex *trans*-K[$IrCl_4(CH_3CN)N(O)SCH_2Ph$] (complex **1b**) seemed to be easier to obtain and characterize than K_2[$IrCl_5N(O)SPh$] (complex **1a**). In fact, after recrystallyzation of **1b** from acetonitrile solution, dark red crystals suitable for X-ray diffraction were obtained[13] (Figure 1a).

The tetraphenylphosphonium salt was also obtained; a saturated aqueous solution of the crude product was added to an ethanol-saturated solution of tetraphenylphosphonium chloride. After slow evaporation of the supernatant, green crystals appeared (**1c**; Figure 1b). Two molecules of water per molecule of **1c** could be seen in the X-ray structure.

In the case of phenylthiol, when the reaction was done at room temperature, the *trans*-K[$IrCl_4(CH_3CN)N(O)SPh$] (complex **2b**) complex was obtained. When carrying the same reaction at a lower temperature, clean formation of K_2-[$IrCl_5N(O)SPh$] (complex **2a**) also occurred.

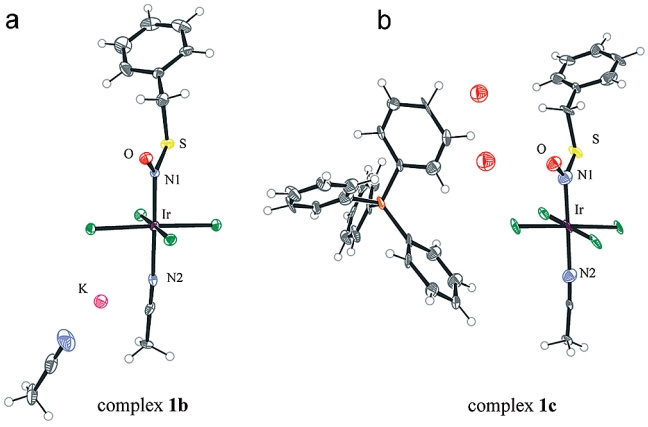

Figure 1. X-ray crystal structures for complexes **1b** with an acetonitrile molecule as solvate and **1c** with two molecules of water. Thermal ellipsoids at the 50% level.

Table 1. Energy of Formation for Complexes **1a**,**b** and **2a**,**b** in the Gas Phase and in Acetonitrile[a]

complex	energy (kcal/mol)	energy (kcal/mol) PCM
1a	15.36	−39.79
1b	−18.51	−44.09
2a	32.10	−31.59
2b	−3.77	−34.29

[a] Zero-point and thermal corrections are included.

In order to gain further insight into the thermodynamic stability of the different products obtained from each thiol, DFT calculations were done in the gas phase and in CH_3CN using the PCM model (see Table 1). We have computed the energy associated with the following reactions:

$$RS^- + [IrCl_5NO]^- \rightarrow [IrCl_5N(O)SR]^{2-} \quad \text{(complexes } \mathbf{a}\text{)} \tag{1}$$

$$RS^- + [IrCl_5NO]^- + CH_3CN \rightarrow$$

$$\textit{trans}\text{-}[IrCl_4(CH_3CN)N(O)SR]^- + Cl^- \quad \text{(complexes } \mathbf{b}\text{)} \tag{2}$$

The differences in energy in the gas phase and in acetonitrile indicate that, for both thiols, the formation of complexes **b** is thermodynamically favored over that of complexes **a**. A more realistic picture is obtained taking into account solvation effects. While in the gas phase the energy difference between complexes **b** and **a** is 33.8 kcal/mol for **1** and 35.8 for **2**, in acetonitrile this difference is much smaller, being only 4.3 and 2.7 kcal/mol, respectively.

Although complexes **a** are less stable than complexes **b**, at low temperatures it is possible to obtain them in the pure form due to their rapid precipitation. At room temperature (∼25 °C), and after a long time (1–2 h), only complexes **b** are obtained, and at temperatures within −20 and +25 °C, mixtures of both **a** and **b** products are obtained.

Biologically Relevant Thiols. We have chosen N-acetyl-L-cysteine and L-cysteine ethyl ester, because of their better solubility in organic solvents than the parent compound cysteine. In addition, these thiols are biologically relevant model thiols. We have recently obtained the coordinated S-nitrosogluthatione (complex **7a**); we have characterized it through UV–visible, FTIR, and ^{1}H NMR spectroscopy, but we have not performed a complete characterization yet.

The reactions were done in a mixture of solvents to improve solubility of the thiols. In the case of N-acetyl-L-cysteine and L-cysteine ethyl ester, the reaction solvent consisted of a mixture of dry MeOH and CH_3CN (∼20 μL/0.25 mL). When the reactions were done at low temperatures, the complexes KH[$IrCl_5N(O)SCH_2CH(NHCOCH_3)COOH$] (complex **3a**) and H[$IrCl_5N(O)SCH_2CH(COOCH_2CH_3)NH_3$] (complex **4a**) were the only products obtained as green precipitates. When the reactions were done at room temperature, the same products were obtained. These products were insoluble in acetonitrile and very soluble in water. When the reaction was done with glutathione, the mixture of solvent used consisted of water and acetonitrile. A stoichiometric amount of trifluoracetic acid was used in order to diminish

Table 2. Energy of Formation for Complexes **5a** and **6a** in the Gas Phase and in Acetonitrile[a]

complex	energy (kcal/mol)	energy (kcal/mol) PCM
5a	18.96	−37.29
6a	20.13	−37.17

[a] Zero-point and thermal corrections are included.

the nucleofilic character of the amines and carboxylic moieties. The complex isolated as a green powder (complex **7a**) turned out to be very stable in the solid form, insoluble in acetonitrile, and very soluble in water.

Mercaptosuccinic Acid and Mercaptosuccinic Acid Methyl Ester. The $[Fe(CN)_5N(SR)O]^{3-}$ complex (complex **5n**, SR = mercaptosuccinate) is reported to be the most stable of the ones derived from nitroprusside ($[Fe(CN)_5NO]^{3-}$), with a lifetime of 36 h.[18] In our case, the reaction of $K[IrCl_5NO]$ with mercaptosuccinic acid dissolved in acetonitrile resulted in a very low yield of product $[IrCl_5N(O)SCH(COOH)CH_2COOH]^{2-}$ (complex **5a**), among other unidentified products. It is possible that the thiol also reacts with $K[IrCl_5NO]$ via the −COOH moieties, leading to the formation of a byproduct. The formation of dimers could also occur.

Esterification of the −COOH moieties and reaction with $K[IrCl_5NO]$ in acetonitrile led to the clean formation of $K_2[IrCl_5N(O)SCH(COOCH_3)CH_2COOCH_3]$ (complex **6a**) as the only product, which precipitated as a green powder. As in the case of the cysteine derivatives, this complex was very soluble in water and insoluble in acetonitrile.

In Table 2 are shown the energies corresponding to the reaction shown in eq 1 for complexes **5a** and **6a** from $[IrCl_5NO]^{2-}$ and RS^- in the gas phase and in CH_3CN. The values obtained show that the thermodynamic stability in the gas phase and in solution is almost the same for both complexes. These results confirm our suggestion that derivatization decreases the reactivity of the product by blocking side reactions in which the carboxylic moieties may be involved, but the intrinsic stability is almost the same. The values also show that formation of the complexes is more favorable in solution than in the gas phase, as the product is more strongly solvated than the reactants.

2. Spectroscopic Properties and Structure of *S*-Nitrosothiol Complexes. Crystallographic Structure. We were able to crystallize the complex bearing **1** with two different counterions: potassium (K^+), when the crystals were obtained from slow evaporation of an acetonitrile solution (complex **1b**), and tetraphenylphosphonium (PPh_4^+), when the cristallyzation was done in water (complex **1c**). It is interesting to mention that the same anion crystallized with a different counterion has a different color, being red when the counterion is K^+ and green for the case of PPh_4^+. Figure 1 shows clearly that both complexes are almost identical from a structural point of view. In addition, all bond lengths are shorter for the PPh_4^+ complex. This fact is in agreement with the corresponding FTIR frequency values (Table 4). The same trend is observed for the selected angles (Table SI1, Supporting Information).

According to the X-ray data, several noticeable features arise:

When the counterion is K^+, the crystal lattice is less sterically crowded than when the counterion is the larger PPh_4^+. This is consistent with the contracted geometry for complex **1c** as compared to **1b**. In addition, in the case of **1c**, the complex has almost a C_s symmetry, while **1b** has a lower symmetry (see Figure 2). The difference in color could be ascribed to the interaction of two of the chloride ligands, with the acceptor K^+ in the case of **1b** (Cl^-−K^+: 3.1 Å) and one chloride ligand with the donor oxygen atoms of two water molecules in the case of **1c** (Cl^-−OH_2: 3.2 Å)(Figure 1).

In the case of complex **1c**, it is important to notice the way in which the PPh_4^+ cation accommodates; instead of placing one above the other as in the case $PPh_4[IrCl_5NO]$,[19] it prefers to form a helix via $\pi-\pi$ ring interactions with itself and the complex.

UV–Visible Characterization. In all cases, the UV/visible absorption consists of four bands: two bands in the UV and two in the visible region; in Figure 3a, the complete spectra for complexes **1a** (green) and **1b** (red) and the reactant $K[IrCl_5NO]$ (ochre) can be seen on a molar absortivities scale. The complex bands are clearly different from the reactant ones (Figure 3a, in ochre). In Figure 3b is shown the UV–visible absorption spectrum for the reactant $K[IrCl_5NO]$, together with the assignation for the bands. The band assignation for the $[IrCl_6]^{-3}$ complex[20] is shown in Figure 3c as a reference. The extinction coefficients are shown for each band inside brackets.

As can be seen in Table 3, all complexes exhibit similar and characteristic spectra. The intense band at 205–260 nm ($\epsilon \sim 10^4$ M^{-1} cm^{-1}) is attributed to the $\pi \rightarrow \pi^*$ transition in the ligand and the Ir−Cl ligand-to-metal charge transfer transition. The next band, centered at about 325–330 nm (ϵ within 1800–4000 M^{-1} cm^{-1}) is assigned to an allowed $n_O \rightarrow \pi^*$ transition in the ligand. There are two other bands in the visible region, one at about 380–400 nm (ϵ within 3000–5000 M^{-1} cm^{-1}) and the other at about 470–580 nm (ϵ within 600–1000 M^{-1} cm^{-1}), both assigned to metal-to-ligand charge transfer (MLCT) transitions. DFT calculations predict the highest occupied molecular orbital (HOMO) to be mainly located on the metal, but with an important contribution of equatorial chlorides (d_{xy}, p(Cl)) and the lowest unoccupied molecular orbital (LUMO) mainly located on the ligand with some choride and acetonitrile contribution; see Figure 4.

Consistently with our tentative assignation, the lowest energy band in the UV–visible spectrum could be qualitatively assigned as (MLCT) transition. This last band is responsible for the color of the *S*-nitrosothiol; the energy of this transition is slightly affected by the thiol structure and by the nature of the solvent. The shoulder observed on this band can be attributed to the existence of two rotational

(18) Szacilowski, K.; Chmura, A.; Stasicka, Z. *Coord. Chem. Rev.* **2005**, *249* (21–22), 2408–2436.

(19) Doctorovich, F.; Di Salvo, F.; Escola, N.; Trapani, C.; Shimon, L. *Organometallics* **2005**, *24* (20), 4707–4709.

(20) Lever A. B. *Inorganic Electronic Spectroscopy*; 2nd ed.; Elsevier: New York, 1984.

Table 3. Selected Experimental Bond Lengths (Å) and IR Frequencies for Complexes Bearing **1**−**6**[a]

species	S1−N2	N2−O2	Ir−N1	Ir−N2	O1−N1−S−C	IR frequencies N−O	S−N	CN
$K[IrCl_5NO]$		1.120[19] (1.170)	1.760[19] (1.755)			2006[19] (1927)		
$Na[IrCl_5NO]$		1.153	1.750			1986		
1-NO	(1.905)	(1.222)				1500–1530[23] (1548)	− (647)	
complex **1a**	(1.990)	(1.238)	(1.894)		(16.28)	1431 (1491)	779 (727)	
complex **1b**	1.734(8) (1.855)	1.219(10) (1.242)	1.963(8) (1.925)	2.032(10) (1.990)	−0.3(8) (0.335)	1432 (1479)	794 (784)	2327 (2446)
complex **1c**	1.659(13)	1.208(14)	1.944(12)	1.983(13)	1.7(13)	1436	852	
complex **1d**						1405	787	
2-NO	(1.918)	(1.216)				1580–1670[23] (1560)	− (649)	
complex **2a**	(2.074)	(1.224)	(1.887)		(13.28)	1438 (1453)	763 (688)	
complex **2b**	(1.917)	(1.229)	(1.923)	(1.989)	(0.644)	1453 (1433)	786 (756)	2324 (2448)
3-NO	(1.945)	(1.211)				(1597)	(622)	
complex **3a**	(1.934)	(1.240)	(1.910)		(40.31)	1431 (1483)	781 (730)	
4-NO	1.769(3)[27] (1.980)	1.191(4)[27] (1.206)				1556 (1616)	637 (649)	
complex **4a**	(1.999)	(1.244)	(1.892)		(11.95)	1438 (1459)	784 (720)	
5-NO	(1.921)	(1.218)				(1567)	(659)	
complex **5a**	(2.007)	(1.239)	(1.886)		(33.82)	1435 (1500)	781 (732)	
6-NO	(1.916)	(1.219)				(1562)	(664)	
complex **6a**	(1.995)	(1.240)	(1.889)		(27.13)	1437 (1493)	790 (736)	
complex **7a**						1422	770	
CH_3CN								2254 (2326)

[a] The DFT calculated values are given in parentheses. X-NO, where X = **1**−**7** denotes the free *S*-nitrosothiol derived form the corresponding thiols **1**−**7**. Note: the FTIR assignation made for **1b** in the previous work[13] corresponds to complex **1a** instead of **1b**.

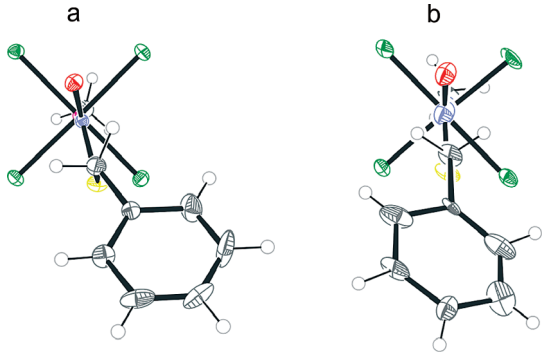

Figure 2. X-ray crystal structures for complexes **1b** (a) and **1c** (b) showing the symmetry adopted.

isomers of the molecule as have been shown to exist in free *S*-nitrosothiols.[21] These visible bands present some solvent dependence, shifting to the blue in the presence of polar solvents (Figure 3a, inset).

The observed solvatochromic effect can be ascribed to an interaction of the chloride ligands with the solvent, similarly to the previously suggested interaction of the cyanide ligands with the solvent in the case of $[Fe(CN)_5NO]^{2-}$,[22] where the cyanides donate charge to the water molecules.

As can be seen in Figure 3a, the spectra for complex **1a** differs slightly from that of complex **1b**; the bands in the visible region are shifted to the blue for complex **1b**, and the shape of the lowest-energy band changes. In addition, a solvatochromic effect could also be observed. In the inset of Figure 3a are shown the spectra for complex **1b** in acetonitrile and in acetone; the lowest-energy band is shifted to the red on going from water to acetonitrile (573 nm) and acetone (583 nm). Another interesting point is that there is only one band in that region of the spectrum, while in water, two bands are observed. The same features are observed for the other complexes.

FTIR Characterization. The experimental and calculated structural parameters and IR vibrations for all complexes studied are listed in Table 4. All complexes studied exhibit two characteristic IR signals. The FTIR spectra were obtained in the solid state, and the assignment of the characteristic bands due to the −SNO group was confirmed by preparing the ^{15}N-labeled derivatives $[IrCl_5{}^{15}N(O)SR]^{2-}$. The difference spectra revealed isotope-sensitive vibrations at about 1405–1438 cm^{-1} and 761–794 cm^{-1}. These bands were attributed to υ(NO) and υ(NS) stretching vibrations, respectively. An important observation is the complete loss of the υ(SH) stretch at approximately 2600 cm^{-1} upon the formation of the *S*-nitroso complex.

Because of their high reactivity, some of the free RSNOs studied here have never been isolated, and in some cases, only a characteristic broad, strong IR band has been assigned to the stretching vibration of N−O. This υ(NO) stretching vibration becomes 70–200 cm^{-1} lower upon coordination. This trend is well described by the calculations that predict a 60−157 cm^{-1} shift toward lower frequencies for the υ(NO) stretching vibration and 40−137 cm^{-1} toward higher frequencies for the υ(SN) stretching vibration.

Complexes bearing **1** and **2** display special features; when acetonitrile is coordinated in the position trans to the RSNO ligand (complex **1b**), the peaks that correspond to the coordinated CN stretching mode vibration are observed at about 2327 cm^{-1}, while for free acetonitrile, they are at 2254 cm^{-1}. These peaks are not observed for complexes **a**. The

(21) Barrett, J.; Debenham, D. F.; Glauser, J. *Chem. Commun.* **1965**, *12*, 248.
(22) Estrin, D. A.; Hamra, O. Y.; Paglieri, L.; Slep, L. D.; Olabe, J. A. *Inorg. Chem.* **1996**, *35* (23), 6832–6837.
(23) Oae, S.; Kim, Y. H.; Fukushima, D.; Shinhama, K. *J. Chem. Soc., Perkin Trans. 1* **1978**, *9*, 913–917.
(24) Patel, R. P.; McAndrew, J.; Sellak, H.; White, C. R.; Jo, H. J.; Freeman, B. A.; rley-Usmar, V. M. *Biochim. Biophys. Acta* **1999**, *1411* (2–3), 385–400.
(25) Moynihan, H. A.; Roberts, S. M. *J. Chem. Soc., Perkin Trans. 1* **1994**, *7*, 797–805.
(26) Clancy, R.; Cederbaum, A. I.; Stoyanovsky, D. A. *J. Med. Chem.* **2001**, *44* (12), 2035–2038.
(27) Yi, J.; Khan, M. A.; Lee, J.; Richter-Addo, G. B. *Nitric Oxide* **2005**, *12* (4), 261–266.

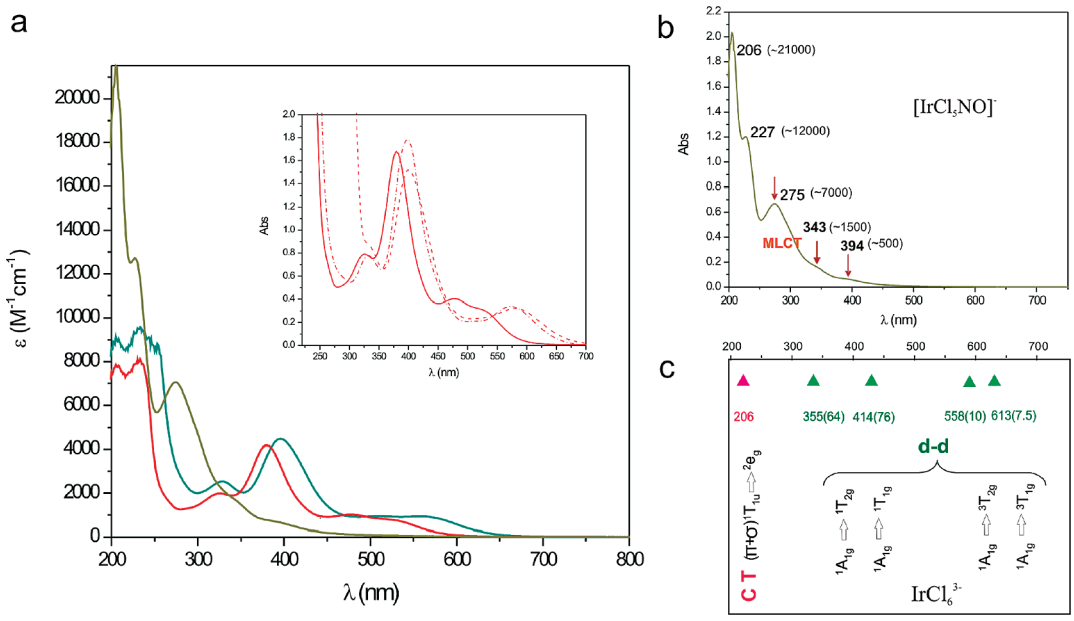

Figure 3. (a) UV–vis spectra for product **1a** ([**1a**] = 3.5 × 10^{-4} M, green line) and **1b** ([**1b**] = 5.1 × 10^{-4} M, red line) in water and reactant K[$IrCl_5NO$] ([K[$IrCl_5NO$]] = 1 × 10^{-3} M, ochre line) in acetonitrile. Inset: product **1b** in water (red line), in acetonitrile (red dot line), and in acetone (red dashed line). (b) UV–vis absorption spectra for the reactant complex K[$IrCl_5NO$] in acetonitrile (λ_{max} are depicted in black, extinction coefficients inside brackets). (c) Spectroscopic assignation for K_3[$IrCl_6$] (charge transfer in pink, d−d transitions in green).

Table 4. UV–Visible Spectroscopic Properties of Complexes Bearing **1**−**6** and the Corresponding Free *S*-Nitrosothiols in Water[a]

complex	λ_{max}, nm (ϵ_{max}, M^{-1} cm^{-1})	S-nitrosothiol	λ_{max}, nm (ϵ_{max}, M^{-1} cm^{-1})
1a	328(2465), 397(4409), 511(876), 556(855)	**1**	340(1020), 530sh(17), 560(26)[23]
1b	325(1809), 387(3883), 475(1059), 525sh(919)		
2a	337(2967), 396(4054), 506(849), 556(822)	**2**	374(1776), 570(53)[24]
2b	325(2821), 387(4728), 478(1174), 525sh(986.6)		
3a	331(2246), 398(4375), 572(944)	**3**	334(507), 545(16)[25]
4a	327(1836), 400(3235), 581(658)	**4**	343(1019), 544(36)[26]
5a[b]	332(2592), 401(5141), 581(1063)	**5**	336(840), 546(13)[5]
6a	322(4801), 397(5674), 574(1358)	**6**	

[a] See Supporting Information for UV–visible spectrum of complex **7a**. [b] Measured in acetonitrile.

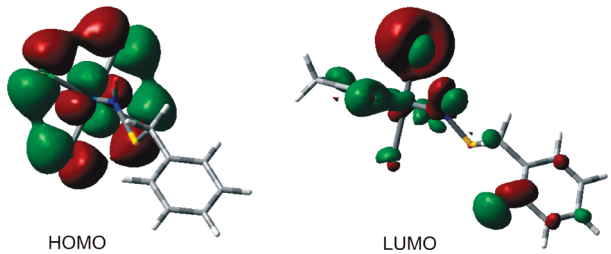

Figure 4. Calculated HOMO and LUMO orbitals for complex **1b**.

υ(NO) stretching vibration has almost the same value for complexes **a** and **b**, while the υ(SN) stretching vibration for complexes **a** is shifted toward lower values, indicating a weakening of the SN bond; this finding is consistent with the calculated thermodynamic stability (Table 2).

In addition, the vibration modes related to S−N and N−O bonds are very sensitive to a change of counterion. As can be observed in Table 4 for complex **1c** ($P(Ph)_4^+$ is the counterion), the N−O and S−N frequencies are shifted to higher values as compared to complexes **1a** and **1b** (K^+ is the counterion). If the counterion is Cs^+ (complex **1d**), the NO frequency is shifted to a lower value (1405 cm^{-1}), while the SN turned out to be 787 cm^{-1}.

The experimental S−N bonds are about 0.1 Å shorter than calculated (Table 4), while the calculated N−O bonds are longer. Thus, at the PBE1PBE/SDD level of theory, the degree of S−NO interaction is underestimated. It is interesting to remark that, when adding polarization functions, geometrical parameters and calculated frequencies matched worse than when using a base such as SDD (without polarization functions; see Supporting Information). It is important to notice some features from this table: upon coordination, the NO distance increases from 1.17 for the K[$IrCl_5SN$] to almost 1.24 for the RSNO complexes. The S−N distance increases for **a** complexes and decreases for **b** ones compared to the free RSNO. Noticeably, the corresponding stretching vibration does not seem to reflect the changes. This fact could be explained taking into account that, upon coordination, the new vibration mode involves not only the S−N bond but also the Ir−NO bond. As depicted in the table, the Ir−NO bond distance is lower for the **a** complexes than for the **b** ones; as mentioned before, the opposite trend is observed for the S−N bond distances in these complexes.

In complexes **b**, the calculations predict that the CN stretching frequency for the coordinated acetonitrile molecule is shifted 120 cm^{-1} toward higher frequencies upon coordination. This is consistent with the experimental value of 70 cm^{-1} toward higher frequencies. As was observed in the

case of the S–N bond, this shift to higher frequencies does not correlate with the measured bond distances for free versus coordinated acetonitrile (1.129 Å versus 1.138 Å (**1b**) and 1.131 Å (**1c**)). When acetonitrile is coordinated to iridium, the CN bond distance is slightly longer than the same distance for the free one. Thus, in this case, the FTIR frequencies do not correlate with the X-ray bond distances; this is probably related to the fact that, upon coordination, the normal mode includes not only the C−N stretching but also the Ir−N one.

ESI-MS Spectra Determination (Complexes 1, 2, 4). Short-lived adducts from the reaction of $[Fe(CN)_5NO]^2$ with thiolates, in particular, mercaptosuccinate, have been previously detected through the ESI-MS technique.[28] The $\{M^+_3[Fe(CN)_5NO(C_4H_4O_4S)]^{4-}\}^-$ ion itself has been identified by MS and also through its decomposition products. In contrast to the above-mentioned case, where the complex is an unstable adduct which could only account for its existence as a minor species, several diagnostic ions could be observed for the iridium complexes, and these ions clearly confirm the identity of the organic ligands and the proposed structures.

All complexes (**1**, **2**, **4**) with coordinated RSNOs provide clean ESI-MS nearly free of fragment ions.

$[IrCl_5N(O)R]^{-2}$ Complexes ($[IrCl_5N(O)SR]^{2-}$ = M; K^+, H^+ = Counterions). For all **a** complexes, $[IrCl_5(NO)]^-$ or $[M - (RS^-)]^-$ (*m*/*z* 399.800) and other anions related to it such as $[IrCl_4]^-$ (*m*/*z* 332.850) have been observed as major ions (see Supporting Information). Considering the stability of the +3 oxidation state for iridium, we assume that the metal remained unaltered as Ir(III).

The major diagnostic anions (those that confirm the identity of these complexes) are $[M - Cl]-$, $[M - Cl - NO]^-\bullet$, and $[M + K]^-$. The ESI-MS spectra of the complexes bearing **1** and **2** (Table SI2, Supporting Information) indicate that only complexes **1a** and **2a** are present due to the single detection of the $[Cl_5Ir\ N(O)SR]^{2-}$ anion; $[Cl_4(CH_3CN)N(O)SR]^-$ was not detected.

According to the spectra, complexes **1a** and **2a** seem to be more stable in the gas phase than complex **4a**. For this complex, only a very small signal for $[M + K]^-$ could be observed, and the signal due to $[M - Cl - K]^-$ was also very small.

The ESI-MS/MS spectra of these complexes show a loss of NO and Cl^- in all cases. An interesting point to remark upon is that, for complexes **1a** and **2a**, the signal related to the $[IrCl_4]^-$ ion is hardly noticeable, but in the case of **4a**, it could be seen with considerable intensity. These findings also suggest the lower stability of **4a** in the gas phase when compared to **1a** and **2a**.

trans-$[IrCl_4(CH_3CN)N(O)R]^{-1}$ Complexes ($[IrCl_4(CH_3CN)N(O)SR]^{1-}$ = M; K^+ or H^+= Counterions). For the **b** complexes, in contrast to what has been observed for complexes **a**, $[M]^-$ and $[M - CH_3CN]^-$ have been observed as major ions; $[IrCl_4\ (CH_3CN)\ (NO)]\bullet^-$ (*m*/*z* 403.797), $[IrCl_5(NO)]^-$ (*m*/*z* 399.800), and other anions related to it such as $[IrCl_4]^-$ (*m*/*z* 332.850) have been observed as minor ions (see Supporting Information). The ESI-MS spectra of these complexes also show that the loss of NO and $[IrCl_4]^-$ is hardly noticeably.

Table 5. Half-Lives Measured for Complexes of the Type *trans*-$[IrCl_4(CH_3CN)N(O)SR]^-$ and $[Fe(CN)_5N(O)SR]^{3-}$, in Water Solution and in the Absence of Oxygen

thiol (R)	τ½ $[IrCl_5N(O)SR]^{2-}$ (min)[a]	τ½ $[Fe(CN)_5N(O)SR]^{3-}$ (min)[b]
1	**1a**, 1.60×10^4	
	1b, 1.99×10^4	
2	**2a**, 1.63×10^3	
	2b, 5.55×10^3	
3	**3a**, 7.75×10^3	**3n**, 7.5[29]
4	**4a**, 2.15×10^2	**4n**, 1.16[29]
5	**5a**, 6.14	**5n**, >2166[29]
6	**6a**, 9.60	

[a] Isolated complex in MilliQ water; pH = 5 for **1**, **2**, and **3**; pH = 4 for **4**, **5**, and **6** (T = 25 °C, *trans*-$[IrCl_4(CH_3CN)N(O)SR]^{2-} \sim 3 \times 10^{-4}$ M). Decomposition was followed at the lowest UV–visible energy band. [b] Complex generated *in situ* from $[Fe(CN)_5NO]^{2-} = 2.5 \times 10^{-3}$ M; thiolate, 1.25×10^{-2} M; Na_2CO_3/H_3BO_3; buffer pH = 10.

^{1}H NMR Characterization. S-nitrosation results in ^{1}H NMR chemical shift changes for the α and β hydrogens with reference to pure thiols. The signals due to the hydrogen atoms located in the α position are shifted downfield, approximately by 1 ppm, while the influence on β hydrogen atoms depends on the structure of the carbon backbone (0.1–0.2 ppm).

Clean ^{1}H NMR spectra were obtained for complexes **1a**,**b**, **2a**,**b**, and **3a** in D_2O. For complexes **1b** and **2b**, coordinated CH_3CN was clearly observed. In the case of complexes **4a** and **7a**, the spectra showed a small amount of disulfide, a product from decomposition. For complexes bearing **5** and **6**, it was not possible to obtain clean spectra in D_2O, since NMR signals attributable to decomposition products immediately appeared and several signals attributable to coordinated CH_3CN were also observed. Cleaner spectra were obtained in DMSO-d_6, where decomposition products could still be observed but in a lower ratio than in D_2O, see Supporting Information.

3. Stability in Water. Half-Lives Measurements. All synthesized complexes turned out to be very stable in the solid form, in the absence of light and oxygen. The thermal stability in water solution depends strongly on the thiol structure. The half-lives of these complexes, in the absence of light, vary from minutes to days even in the presence of oxygen. In all cases, except for complexes **1b** and **2b**, the decomposition obeys first-order kinetics. Oxygen seems to have no effect on the reaction rate in all cases.

Table 5 depicts the half-lives measured for the iridium complexes together with previously measured values[5,18] for $[Fe(CN)_5N(O)SR]^{3-}$ complexes.

Complexes **1a**,**b** are the most stable of all studied complexes. When dissolved in water, they can be stored in the dark and at low temperatures for several months. Complexes **2a**,**b** and **3a** are also very stable. In the case of

(28) Lawrance, G. A.; Maeder, M.; Neuhold, Y. M.; Szacilowski, K.; Barbieri, A.; Stasicka, Z. *J. Chem. Soc., Dalton Trans.* **2002**, *19*, 3649–3655.

(29) Szacilowski, K.; Stochel, G.; Stasicka, Z.; Kisch, H. *New J. Chem.* **1997**, *21* (8), 893–902.

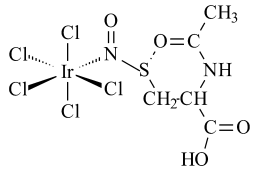

Figure 5. Intermolecular stabilization of the coordinated N-acyl-S-nitrosothiol **3a**.

complexes **3a** and **4a**, it is important to notice the huge increase in stability of the coordinated *S*-nitrosothiol as compared to $[Fe(CN)_5N(O)SR]^{3-}$ complexes. Although both complexes **3a** and **4b** involve *S*-nitrosothiols derived from cysteine, complex **4a** is less stable than **3a**; the same trend is observed for nitroprusside complexes; for the latter, it has been suggested that the formation of a six-membered ring by the N-acyl thiols in solution probably[12] results in a strengthening of the S−N bond at the expense of a weakening of the N−O bond. As alluded to above, this effect may contribute to the increased stability, see Figure 5.

As previously mentioned, the decomposition of complexes **1b** and **2b** did not obey first-order kinetics; these complexes turned out to be more stable in water than the respective **a** complexes.

Complexes bearing **5** and **6** deserve special attention; contrary to what has been observed for the $[Fe(CN)_5N(O)SR]^{3-}$ complex **5n**, the iridium ones are by far the most unstable of all, with half-lives of 6 and 9 min, respectively. In the case of **5n**, the presence of the electron-attracting carbonyl group β to the *S*-nitrosothiol group probably stabilizes the RSNO ligand by making it less prone to oxidation. However, in the case of **5a**, the carbonyl group competes with the electrophilic $[IrCl_5]^{-2}$ moiety, diminishing its stabilizing effect.

In order to gain further insight, we have also performed calculations on $[Fe(CN)_5N(SR)O]^{3-}$ (RS^- = mercaptosuccinate), complex **5n**. Importantly, we found that this complex as such is not a minimum in the gas phase. When optimization was done, cleavage of the N−S bond occurred, leading to thiolate and $[Fe(CN)_5NO]^{2-}$. The situation changes by adding one or more water molecules close to the cyanide moieties (see Figure 6). The S−N bond distance in this complex turns out to be 2.17 Å, while the same parameter for the iridium complexes is 2.00 and 1.99 (Table 4).

We also performed calculations with methylthiol as a model thiol, for the nitroprusside complex (**8n**) and iridium complexes **8a** and **8b**. As can be observed in Table 6, the S−N bond distance is 0.3–0.4 Å larger for the nitroprusside complex as compared to that of **8a**. Additionally, the natural bond order (NBO) charges, especially on the sulfur atom, show that in the case of complexes **8a** and **8b** the *S*-nitrosothiol is coordinated, but in the case of **8n**, the slightly negative charge on sulfur indicates that, instead of having the coordinated *S*-nitrosothiol, the nitroprusside is interacting with the thiolate.

These findings again point toward the fact that the solvent plays an important role in the stability of the **n** complex; in fact, it has been suggested that interaction of cations with complex **5n** stabilizes the S−N bond, changing the charge

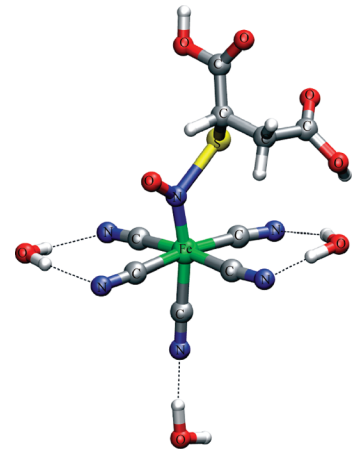

Figure 6. Optimized geometry of $[Fe(CN)_5N(SR)O]^{3-}$ (RS^- = mercaptosuccinate) in the gas phase, with three molecules of water-solvating cyanides.

Table 6. Calculated Structural Parameters and NBO Charges for Optimized Model Complexes

	distances (Å)			NBO charges (*e*)		
complex	S−N	N−O	Fe/Ir−N	S	N	O
8n	2.244	1.220	1.759	−0.109	0.284	−0.318
8a	1.939	1.243	1.901	0.263	0.035	−0.308
8b	1.854	1.240	1.920	0.403	0.014	−0.269

distribution in the complex.[29,30] This in turn increases the complex stability in the presence of cations forming stable ion pairs.

Observed Decomposition Products through ^{1}H NMR, UV–Visible, and X-ray Crystallography. In all cases, as the decomposition proceeds, disulfide and complexes of the type $[IrCl_5\text{-}nX_nSolv]^{-(2-n)}$, where the iridium oxidation state seems to remain unchanged, are formed. The $[IrCl_5\text{-}nX_nSolv]^{-(2-n)}$ complexes show UV–visible spectra which are characteristic of iridium complexes, where the oxidation state is Ir(III), see Figure SI2 in the Supporting Information.[31] Only disulfide formation as the organic product was detected by ^{1}H NMR after complete decomposition (see Figures SI3 and SI4, Supporting Information). In the case of complex **6**, other unidentified products were also observed. In some cases, iridium-coordinated acetonitrile could also be observed (Figure SI4, Supporting Information).

In the case of **2b**, a crystal suitable for X-ray analysis was obtained, and *cis*-$[IrCl_4(CH_3CN)_2]K\cdot 2CH_3CN$ (complex **8**) was observed as the decomposition product in acetonitrile in the absence of light (Figure 7).

It is surprising that the obtained product is the cis and not the trans bis-acetonitrile as expected, since CH_3CN in **2b** is presumably located trans to the RSNO ligand, as in the case of **1b**. This could be rationalized in terms of a mechanism which involves the $[IrCl_4(CH_3CN)]^-$ intermediate with a trigonal bipyramid geometry.

4. General Remarks. Up to this point, a complete characterization and discussion of several properties of these complexes has been done. As a result of trying to integrate and rationalize the observed properties, general remarks arise.

(30) Szacilowski, K. *Chem.—Eur. J.* **2004**, *10* (10), 2520–2528.
(31) Chang, J. C.; Garner, C. S. *Inorg. Chem.* **1965**, *4* (2), 209.

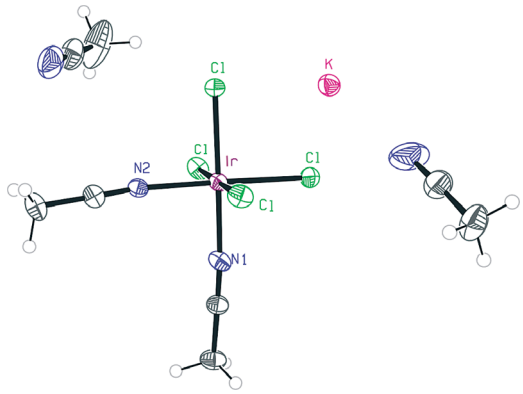

Figure 7. X-ray crystal structure of *cis*-[$IrCl_4(CH_3CN)_2$]K·2CH_3CN (**7**). Thermal ellipsoids are shown at the 50% level.

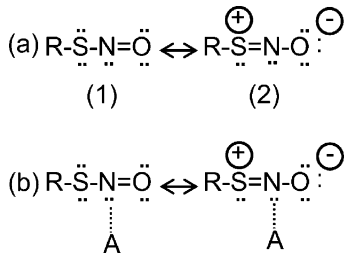

Figure 8. Resonance structures for (a) free RSNO and (b) its complexes with a Lewis acid (A) such as a metal ion.

If we describe the electronic structure of free RSNOs as a combination of two resonance structures (Figure 8a),[32] one (1) is the conventional RSNO structure with a double N−O and a single S−N bond and the other (2) is like a zwitterionic structure that possesses a double S−N and a single N−O bond. In the case of free RSNOs, an electron distribution like 2 would be favored by those substituents which donate electron density, strengthening the S−N bond and weakening the N−O bond. The opposite effect is achieved with withdrawing substituents; in this case, the electron density is shifted within the thiolate moiety due to the inductive effect of the substituent.[33]

If we consider the interaction of RSNOs with a Lewis acid, A (Figure 8b), through its nitrogen atom, the result would be the same as having an electron-releasing substituent (R). An electron shift from the lone pairs localized at the sulfur atom toward A would be favored, thus generating a local positive charge on the sulfur atom, strengthening the S−N bond. The observed increase in stability for the coordinated *S*-nitrosothiols could be explained in terms of the above-mentioned facts where A is now the iridate moiety $[IrCl_5]^{2-}$. The intrinsic stability for each coordinated RSNO is also related to the structure of the R substituent. If R is an electron-releasing substituent, the stability would be enhanced, whereas the opposite would occur if R is an electron-withdrawing group.

As alluded to above, regarding the stability of these complexes in water, we cannot generalize and explain in terms of a family of compounds because each of them display special features. This is consistent with the strong influence of the thiol structure mentioned previously. All of the complexes turned out to be more stable than the ironpentacyano ones except for the case of mercaptosuccinic acid and mercaptosuccinic methyl ester. This is probably due to the combination of the electrophilic character of the iridium center and the withdrawing effect of the carboxylate moieties, as stated before. It is interesting to remark that, in the case of the ironpentacyano complexes, the electronegative carboxylates deplete electron density from the sulfur atom and inhibit electron transfer to the iron center stabilizing the complex. As a final comment, considering electronic effects, it can be said that the R substituents that stabilize coordinated RSNO iridium complexes unstabilize the ironpentacyano ones.

On the other hand, it has been suggested that conformational flexibility could influence compound stability. In addition, thermal stability may be affected by the steric interactions involved in the formation of disulfide. It is known that for free *S*-nitrosothiols the thermodynamic preferred conformation is rigidly planar, with the anti conformation favored. The difference in energy between the syn and anti conformations appears to be a function of the specific steric constraints for the moiety. There is, however, a substantial barrier for the interconversion of these conformers, and twisting or any disruption of the planarity of this group destabilizes the fragment toward S−N breaking.Remarkably, it could be observed that the calculated C−S−N−O torsion angle is almost zero for **1b** and **2b**; between 11 and 16° for complexes **1a**, **2a**, and **3a**; and between 27 and 40° for the other complexes (see Table 4), indicating more flexibility. On the basis of this evidence, it is quite possible that the conformational dynamics of coordinated RSNOs may also play a role in the stability of these complexes.

Although we have not performed a detailed mechanistic study for the decomposition of the RSNO complexes, the behavior of the RSNO ligand seems to resemble that of its parent nitrosothiol in undergoing probably both heterolytic and homolytic cleavage of the S−N bond: the former is accompanied by the formation of $[IrCl_{5-n}X_nNO]^{-(2-n)}$ and RS^- ions (the inverse reaction of its synthesis), whereas homolytic rupture leads to different possibilities, as shown in Scheme 2. Another decomposition pathway for these complexes could be breakage of the Ir−N bond leading to free RSNO and $[IrCl_5\text{-}nX_nSolv]^{-(2-n)}$.

In Table 7, we show the calculated energies for the possible decomposition pathways, taking as illustrative examples complexes **1a** and **1b**.

The results depicted in Table 7 show that, in the case of **a** complexes in the gas phase, the S−N heterolytic rupture is likely to occur to a greater extent (mechanism II), while in solution, the N−Ir heterolytic rupture, leading to the free RSNO, seems to be the more feasible pathway. In the case of **b** complexes, both in the gas phase and in solution, the Ir−N heterolytic rupture (mechanism I) seems to be the most favorable pathway.

ESI-MS results showed that, in the gas phase, both heterolytic and homolytic decomposition occur. All **a** complexes lose NO, leading to the thiol−iridium com-

(32) Timerghazin, Q. K.; Peslherbe, G. H.; English, A. M. *Org. Lett.* **2007**, *9* (16), 3049–3052.
(33) Arulsamy, N.; Bohle, D. S.; Butt, J. A.; Irvine, G. J.; Jordan, P. A.; Sagan, E. *J. Am. Chem. Soc.* **1999**, *121* (30), 7115–7123.

Scheme 2. Mechanistic Pathways for the Decomposition of Coordinated *S*-Nitrosothiol Complexes[a]

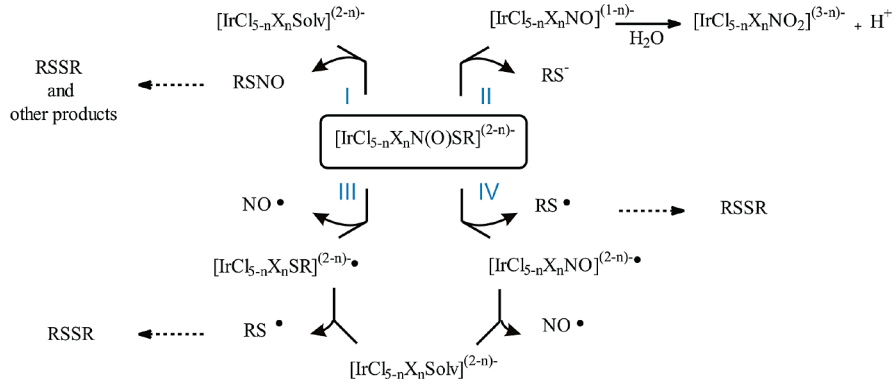

[a] X: CH_3CN molecule; *n* could be 0 or 1.

Table 7. Calculated Energies for the First Step of the Different Mechanisms in kcal/mol[a]

	mechanism I		mechanism II		mechanism III		mechanism IV	
complex	gas phase	(PCM) H_2O	gas phase	(PCM) H_2O	gas phase	(PCM) H_2O	gas phase	(PCM) H_2O
1a	17.27	9.65	−17.28	37.81	17.56	17.66	32.43	34.48
1b	2.46	5.28	72.56	62.68	19.00	22.79	30.80	39.75

[a] All values include zero-point corrections.

plexes which could be observed as $[M-NO-Cl]^{\bullet-}$ ions. The loss of RS• radical leads to ions of the type $[IrCl_4NO]^{\bullet-}$ (362.82 *m*/*z*), which were clearly observed in all cases. While in the gas phase, all of the possible decomposition pathways seem to be operative, some of them to a greater extent than others, depending on the particular complex and kind of product for each complex (**a** versus **b**); in solution, the situation appears to be very different. When the complexes were dissolved in water, disulfide (see Supporting Information, Figures SI3–4) and complexes of the type $[IrCl_5\text{-}nX_nSolv]^{-(2-n)}$ were observed as decomposition products. We did not find clear evidence for the existence of complexes of the type $[IrCl_{5-n}X_nNO]^{-(2-n)}$ or $[IrCl_{5-n}X_nSR]^{-(2-n)}$. It is important to notice that free RSNOs were not observed in the ^1H NMR spectra as the decomposition proceeded, probably because their decomposition rate is faster than their formation rate. In summary, further experiments are necessary in order to rationalize the decomposition pathways in water solution in terms of one or various mechanisms shown in Scheme 2.

Concluding Remarks

A complete characterization has been done for a variety of coordinated *S*-nitrosothiols. This work shows that the very rich chemistry of coordinated *S*-nitrosothiols has its source in the unique properties that result from their coordination to the iridium center Ir(III)Cl_n (n = 4 or 5). All of the complexes turned out to be very stable in solid form, and they can be stored for several months. When dissolved in water in the absence of light, they display a broad range of lifetimes indicating very different reactivity and a strong dependence on thiol structure.

The nature of R appears to be of crucial relevance to the stability, properties, and type of complex obtained (**a** vs **b**). As a consequence, structural changes in the R group provide substantial changes in the complex properties. All complexes turned out to be quite sensitive to environmental effects. For example, complex **1** crystallized as green or red crystals depending on the solvent and counterion. The N−O and S−N bond distances are also very sensitive to changes in the counterion. In addition, all of the complexes display interesting solvatochromic effects.

A very interesting fact is the obtainment of *trans*-$[(CH_3CN)IrCl_4N(O)SR]^-$ complexes; this appears to occur only for thiols with aromatic rings. In these cases, we were able to isolate both complexes *trans*-$[(CH_3CN)IrCl_4N(O)SR]^-$ and $[IrCl_5N(O)SR]^{-2}$ (R = benzyl, phenyl). Labilization of the trans chloride upon ligand coordination may be useful for synthetic purposes and could give also the possibility to tune the coordinated *S*-nitrosothiol stability by selecting a proper trans ligand.

Acknowledgment. The authors thank CONICET, UBA, and ANPCyT for financial support and Professors Marcos Eberlin for MS analysis, David Milstein for X-ray analysis, and especially Jan Martin for providing the SDB-cc-pVDZ basis set.

Supporting Information Available: Complete UV–visible, FTIR, and NMR spectra; ESI-MS; and ESI-MS−MS of the most important ions; computed geometries; geometrical parameters; and crystallographic information files (CIF) are included. This material is available free of charge via the Internet at http://pubs.acs.org.

IC7024999